Biochimica et Biophysica Acta 1857 (2016) 1900–1908

Contents lists available at ScienceDirect

Biochimica et Biophysica Acta

journal homepage: www.elsevier.com/locate/bbabio

Photochemical characterization of actinorhodopsin and its functional existence in the natural host

Shintaro Nakamura [a], Takashi Kikukawa [a,*], Jun Tamogami [b], Masakatsu Kamiya [a], Tomoyasu Aizawa [a], Martin W. Hahn [c], Kunio Ihara [d], Naoki Kamo [a], Makoto Demura [a]

[a] Faculty of Advanced Life Science, Hokkaido University, Sapporo, Japan
[b] College of Pharmaceutical Sciences, Matsuyama University, Matsuyama, Japan
[c] Research Institute for Limnology, University of Innsbruck, Mondsee, Austria
[d] Center for Gene Research, Nagoya University, Nagoya, Japan

ARTICLE INFO

Article history:
Received 21 April 2016
Received in revised form 13 September 2016
Accepted 17 September 2016
Available online 20 September 2016

Keywords:
Actinorhodopsin
Light-driven proton pump
Phototrophy
Photocycle
Flash photolysis
Microbial rhodopsin

ABSTRACT

Actinorhodopsin (ActR) is a light-driven outward H^+ pump. Although the genes of ActRs are widely spread among freshwater bacterioplankton, there are no prior data on their functional expression in native cell membranes. Here, we demonstrate ActR phototrophy in the native actinobacterium. Genome analysis showed that *Candidatus* Rhodoluna planktonica, a freshwater actinobacterium, encodes one microbial rhodopsin (RpActR) belonging to the ActR family. Reflecting the functional expression of RpActR, illumination induced the acidification of the actinobacterial cell suspension and then elevated the ATP content inside the cells. The photochemistry of RpActR was also examined using heterologously expressed RpActR in *Escherichia coli* membranes. The purified RpActR showed λ_{max} at 534 nm and underwent a photocycle characterized by the very fast formation of M intermediate. The subsequent intermediate, named P_{620}, could be assigned to the O intermediate in other H^+ pumps. In contrast to conventional O, the accumulation of P_{620} remains prominent, even at high pH. Flash-induced absorbance changes suggested that there exists only one kind of photocycle at any pH. However, above pH 7, RpActR shows heterogeneity in the H^+ transfer sequences: one first captures H^+ and then releases it during the formation and decay of P_{620}, while the other first releases H^+ prior to H^+ uptake during P_{620} formation.

1. Introduction

Microbial rhodopsins are ubiquitous membrane proteins in unicellular microorganisms [1,2]. They commonly consist of seven transmembrane helices surrounding a chromophore retinal, which binds to a conserved lysine residue in the last helix *via* a protonated Schiff base (PSB; the deprotonated Schiff base is abbreviated as SB). Upon illumination, the retinal undergoes isomerization from an all-*trans* to a 13-*cis* configuration. This change elevates the protein to the excited state, which is thermally relaxed to the original state *via* various photochemical intermediates. During this cyclic reaction, called the photocycle, microbial rhodopsin performs various roles, including light-driven ion pumps, ion channels, and photosensory transductions. In 1971, the first microbial rhodopsin was discovered in an extremely halophilic archaeon, *Halobacterium salinarum*, and named bacteriorhodopsin (BR) [3]. Subsequently, it was proven that BR acts as an outward H^+ pump and can drive cellular ATP synthesis by creating an H^+-electrochemical gradient across the cell membrane [4]. Later, three relatives with different functions were discovered from the same archaeon: inward Cl^- pump halorhodopsin [5], phototaxis sensors sensory rhodopsin I [6], and sensory rhodopsin II (also called phoborhodopsin) [7]. For approximately 30 years, research on microbial rhodopsins was confined to these four archaeal rhodopsins [8]. Since 1999, however, the genes for other microbial rhodopsins have been identified in various microorganisms, including eubacteria, fungi, algae, and even viruses. Some new members have the same functions as the archaeal rhodopsins, whereas others perform novel roles, acting as outward Na^+ pumps [9,10], cation and anion channels [11–14], and sensors for the regulation of gene expression [15]. Thus, microbial rhodopsins are now identified as a large and diverse family.

H^+ pumps define the largest functional class in the microbial rhodopsins and are widespread in various microorganisms inhabiting a broad range of environments. For aqueous environments, their abundances have been clarified through metagenomic analyses. For marine

Abbreviations: ActR, actinorhodopsin; RpActR, ActR from *Candidatus* Rhodoluna planktonica; PSB, protonated Schiff base; SB, deprotonated Schiff base; BR, bacteriorhodopsin; PR, proteorhodopsin; XR, xanthorhodopsin; GR, *Gloeobacter* rhodopsin; CCCP, carbonyl cyanide *m*-chlorophenylhydrazone; DDM, *n*-dodecyl β-D-maltopyranoside; PC, phosphatidylcholine; ITO, indium tin oxide; ORF, open reading frame; ESR, *Exiguobacterium sibiricum* rhodopsin; PRG, H^+-releasing group; EC, extracellular; CP, cytoplasmic.

* Corresponding author at: Faculty of Advanced Life Science, Hokkaido University, N10W8, Kita-ku, Sapporo 060-0810, Japan.
E-mail address: kikukawa@sci.hokudai.ac.jp (T. Kikukawa).

http://dx.doi.org/10.1016/j.bbabio.2016.09.006
0005-2728/

environments, the gene encoding the H^+ pump was first identified in 2000 in a DNA fragment from an uncultivated γ-proteobacterium (the SAR86 group), which is one of the most abundant marine bacterioplankton [16]. This H^+ pump was named proteorhodopsin (PR). The expression of photoactive PR was verified in native planktonic membrane preparations [17]. Later, PR genes were identified in other oceanic microbial groups, and it was established that PR-encoding microorganisms are common in the world oceans (for reviews, see [8,18]). The cellular expression of PR and its H^+-pumping activity were also proven in cultivated host strains. In some strains, light-activated PR conferred observable benefits on the cells, such as growth enhancement, fuel CO_2 fixation, and extended survival under starvation. Functional PR is available from the heterologous *Escherichia coli* system with exogenous retinal [16]. Thus, the photochemistry of PR has been examined in detail (for reviews, see refs [2,19,20]).

For non-marine aqueous environments, metagenomic analysis revealed that a PR-related but phylogenetically distinct gene group is present in high abundance [21]. This predicted H^+-pump group was named actinorhodopsin (ActR) because these genes are exclusively associated with actinobacteria, which are common inhabitants of freshwater environments [22]. Later, ActR genes were indeed found in cultivated freshwater actinobacteria [23] and further identified in other freshwater bacterioplankton [24]. Thus, it is now established that ActR genes are widespread in freshwater environments. In contrast to PR, ActR genes are almost completely absent in marine environments [21].

Despite its broad distribution, ActR has been less well characterized in both its physiological and photochemical aspects. Its broad distribution implies its significant contribution to the solar energy utilization in the environment. However, a previous study was not able to demonstrate the fully functional expression of ActR in the native cells. In actinobacterium *Rhodoluna lacicola* strain MWH-Ta8, the ActR opsin was constitutively expressed but did not contain the retinal [25]. This immature ActR required exogenous retinal to perform the H^+-pumping function. This result was consistent with the fact that *R. lacicola* lacks the gene encoding the homolog of β-carotene cleavage enzyme (β-carotene 15,15′-monooxygenase), which is necessary for the final step of the known retinal biosynthesis process.

In this study, we examined ActR from the freshwater actinobacterium *Candidatus* Rhodoluna planktonica strain MWH-Dar1. Hereafter, this ActR is designated RpActR. The genome analysis showed that this strain encodes the genes for retinal biosynthesis enzymes, including a putative β-carotene cleavage enzyme, and lacks microbial rhodopsin genes other than RpActR. Without the exogenous retinal, RpActR performed outward H^+-pumping activity in the native cell membrane and thus drove ATP production. Thus, this study includes the first observation of ActR phototrophy in native actinobacterial cells. RpActR was also photochemically characterized after heterologous expression in *E. coli* cells. The purified RpActR had a λ_{max} of 534 nm and underwent a photocycle characterized by the very fast formation of M intermediate and prominent accumulation of O-like intermediate (named P_{620}) even at high pH. Together with the observed H^+-transfer reactions, the photocycle of RpActR will be discussed.

2. Materials and methods

2.1. Cultivation and DNA sequence analysis of the actinobacterium

The actinobacterium was grown in 3 g/L NSY medium at pH 7.2 [26]. The culture of strain MWH-Dar1 contained initially a small fraction of non-actinobacterial contamination (<1%) [27]. In order to establish a pure culture, the following purification procedure was performed. First, 5 mL of NSY medium was inoculated with the cells from the agar slant and gently shaken at 28 °C until the stationary phase. After dilution, the cells were plated on NSY agar plate and grown at 28 °C for approximately 4 days. A single colony on the plate was used to inoculate the next 5 mL medium. This purification cycle was performed in triplicate. The new liquid culture started from a single colony on the third plate was mixed with glycerol (15% v/v) and stored at −80 °C. Careful tests in three labs confirmed the purity of the culture. The strain was deposited at the German Collection of Microorganisms and Cell Cultures (DSMZ), Braunschweig, Germany, under the number DSM 103376. The established glycerol stock was used as the seed culture for the following experiments.

For genomic DNA extraction, the cells were grown in 5 mL medium until the stationary phase. The cells were harvested by centrifugation and pretreated with lysozyme to lyse the cell walls. Then, the genomic DNA was extracted using a QIAGEN DNeasy Blood & Tissue Kit (Qiagen, Hilden, Germany) and used for the sequence analysis. The genomic DNA library was constructed using the tagmentation method (Nextera XT, Illumina, San Diego, CA, USA). The obtained library with an average insert size of approximately 1 kbp was selected using AMPure XP beads and sequenced using a MiSeq v3 600PE kit (Illumina). Approximately 5.58 million reads were obtained and assembled using the SPAdes 3.1 software. A single contig of 1.42 Mbp was obtained, and the genome sequence of the strain could be closed. The encoded genes were annotated using the RAST server [28]. The RpActR gene and the complete genome sequence were deposited at DDBJ/EMBL/GenBank under accession numbers LC144836 and CP015208, respectively.

2.2. Proton-pumping activity and ATP content in actinobacteria

Ca. R. planktonica were grown with or without 1 mM nicotine. The cells in glycerol stock were transferred to a tube containing 3 mL liquid medium and shaken at 25 °C for 3 days, then transferred to a 300-mL flask containing 40 mL medium. After 3 days, the culture reached the late exponential phase. The cells were then harvested at 3600 ×g for 5 min at 4 °C and washed twice in basal solution (0.3 g/L NaCl, 0.1 g/L $MgSO_4$) containing no buffering agent. The cells were suspended again in the basal solution and used for the following measurements.

The H^+-pump activity of RpActR was measured at 25 °C using a conventional pH electrode method that detects the light-induced acidification of the cell suspension due to the H^+-pump activity itself. The cell suspension was diluted with basal solution at an A_{660} of 0.5. The pH of this suspension was about 6.5–7.0. For the activation of RpActR, the cell suspension was irradiated with green LED light at 530 ± 17.5 nm (LXHL-LM5C, Philips Lumileds Lighting Co., San Jose, CA, USA). The H^+ transport was examined in the absence and presence of 10 μM carbonyl cyanide *m*-chlorophenylhydrazone (CCCP). The resulting pH changes were converted to the molar amount of transported H^+ by adding known amounts of HCl after each measurement.

To assay the ATP content, the cell suspension was gently shaken overnight at 25 °C. Then, the cells were washed twice and finally suspended at an A_{660} of 0.1 in 10 mM Tris-AcOH, pH 7.8. This cell suspension was kept in the dark until the ATP assay. The ATP inside the cell was extracted using the Kinsiro ATP extraction reagent kit (LL-100-2; Toyo Ink, Tokyo, Japan), and the ATP level was determined using the Kinsiro ATP luminescence kit (LL-100-1; Toyo Ink) according to the manufacturer's instructions. Briefly, 5 μL of the cell suspension was mixed with the same volume of ATP extraction reagent and incubated for 20 s. To examine the effect of RpActR activity, the cell suspension was irradiated for 5 min with green LED light immediately prior to the ATP extraction. After the incubation, the resultant cell lysate was mixed with 100 μL of luciferin/luciferase reaction reagent. Immediately after mixing, the luminescence intensity at 560 nm was integrated for 20 s using a Model AB-2200 luminometer (ATTO, Tokyo, Japan). All procedures except LED irradiation were performed under dim conditions. The integrated luminescence value was converted to the ATP concentration using a standard line, which was constructed from the independent experiments. The total protein concentrations of the original cell

suspensions were quantified using a protein assay kit (PQ02; Dojindo Lab., Kumamoto, Japan).

2.3. Expression, purification and lipid reconstitution of RpActR

Escherichia coli strain DH5α was used for DNA manipulation. To isolate the RpActR gene, PCR was employed on *Ca.* R. planktonica genomic DNA. The sense and antisense primers were 5′–actattgcatatgaattctctttcgtccatc-3′ and 5′–taatctcgaggtcgcggaactcgttcttag-3′, respectively, in which the underlines denote the added restriction enzyme sites for *Nde*I and *Xho*I. The PCR product was then cut using these restriction enzymes, and the resultant DNA fragments were ligated to the *Nde*I/*Xho*I site of the pET-21c (+) vector (Merck). This plasmid results in RpActR having additional amino acids in the C-terminus (-LEHHHHHH). The E103Q mutation was introduced using the QuikChange site-directed mutagenesis kit (Stratagene, La Jolla, CA, USA). The DNA sequences were confirmed by a standard procedure using an automated DNA sequencer (model 3100, Applied Biosystems, Foster City, CA, USA).

E. coli strain BL21(DE3) was used for the expression and purification of RpActR. The procedures were essentially the same as the ones previously described [29]. Briefly, the cells were grown in 2 × YT medium at 37 °C, and expression was induced by the addition of 1 mM isopropyl-β-D-thiogalactopyranoside in the presence of 10 μM all-*trans* retinal. After 4 h of induction, the cells were harvested and broken with a French press. The collected cell membrane fraction was solubilized with 1.5% *n*-dodecyl β-D-maltopyranoside (DDM) (Dojindo Lab., Kumamoto, Japan), and the solubilized RpActR was purified using Ni-NTA agarose (Qiagen, Hilden, Germany). The yield of RpActR was approximately 3.5 mg from 1 L culture. The concentration of RpActR was determined from the absorbance at 534 nm with an assumed extinction coefficient of 40,000 M^{-1} cm^{-1}. The purified samples were replaced with an appropriate buffer solution by passage over Sephadex G-25 in a PD-10 column (Amersham Bioscience, Uppsala, Sweden).

For reconstitution into the lipid, phosphatidylcholine (PC) from egg yolk (Avanti, Alabaster, AL, USA) was added at a RpActR:PC molar ratio of 1:30. The detergent was removed by gentle stirring overnight (4 °C) in the presence of SM2 Adsorbent Bio-Beads (Bio-Rad, Hercules, CA, USA). After filtration, the reconstituted RpActR was collected by centrifugation.

2.4. HPLC analysis

The retinal compositions of RpActR in the dark/light adapted states were analyzed. RpActR was suspended in 10 mM MOPS, pH 7, containing 100 mM NaCl and 0.1% DDM. For dark adaptation, RpActR was kept in the dark for 24 h at room temperature. For light adaptation, the dark-adapted RpActR was irradiated for 5 min with green LED light. The retinal oxime extraction and the subsequent HPLC analysis were performed as previously described [30].

2.5. Absorption spectra measurements and flash photolysis

The UV-visible spectra of RpActR were measured using a UV-1800 spectrometer (Shimadzu, Kyoto, Japan). Solubilized RpActR with 0.1% DDM was suspended in the 6-mix buffer (citric acid/MES/MOPS/HEPES/CAPS/CHES, 1 mM each) containing 100 mM NaCl.

To observe the formation and decay of photo-intermediates, flash-induced absorbance changes were measured. The apparatus equipped with a Q-switched Nd-YAG laser (532 nm, 7 ns) was described previously [31]. At the selected wavelength, 30 laser pulses were used to improve the S/N ratio. The data set, measured from 320 nm to 700 nm with a 10 nm interval, was analyzed based on an irreversible sequential model [32]. The details of the procedure were described previously [33,34]. Briefly, this analysis assumes that the photocycle is represented by the irreversible sequential conversion of the kinetically defined intermediates, such as $P_0 \rightarrow P_1 \rightarrow P_2 \rightarrow \ldots. P_n \rightarrow P_0$, where P_0 represents the original unphotolyzed state. The number of exponents in the fitting equation, given as n, was determined from the reductions in the standard deviation of the weighted residuals. The data weight was determined independently for each wavelength by estimating the average error from the baseline part before flash irradiation (−44 to 0 ms). Using the results from this fit, the time constant (τ_i) and the absorption differences between P_i and P_0 ($\Delta\varepsilon_i$) were calculated. The P_0 spectrum was obtained independently by subtracting the background scattering ($A + B/\lambda^4$; λ in nanometers) from the measured spectrum of the unphotolyzed state. Finally, the absolute spectra of the P_i states were obtained by adding the spectrum of P_0 to the absorption differences ($\Delta\varepsilon_i$). All flash photolysis experiments were performed for the PC-reconstituted RpActR. For the calculation of the P_0 spectrum, we used the spectrum measured in the DDM-solubilized state because the spectrum in the PC-reconstituted state included strong scattering artifact. The samples contained approximately 6 μM RpActR and were suspended in the 6-mix buffer containing 100 mM NaCl. All measurements were performed at 25 °C.

2.6. Measurements of flash-induced proton transfers

The flash-induced H^+ transfer was measured using an indium tin oxide (ITO) transparent electrode, which has been shown to act as a time-resolved pH sensor [35–37]. In this experiment, the PC-reconstituted RpActR was used. To eliminate the salt and buffering agents, the reconstituted sample was washed several times and diluted with distilled water to contain approximately 9 μM RpActR. A 100 μL droplet of this suspension was applied to the surface of the ITO electrodes (Techno Print Co., Saitama, Japan), followed by the evaporation of water under reduced pressure to produce a dried film approximately 10 mm in diameter. Weakly bound proteins were removed by rinsing with distilled water, and then this electrode was placed into the electrochemical cell, in which a buffer solution was sandwiched with two ITO electrodes: one is the ITO adsorbing the protein and the other is bare ITO for the reference electrode. The buffer solution contained 6-mix buffer plus 100 mM NaCl, and the pH was adjusted at desired value. The sample was activated by a 7 ns laser pulse (532 nm, 0.6 mJ/pulse) from a Q-switched Nd:YAG laser (Minilite I, Continuum, San Jose, CA, USA). The electric potential difference between two ITO electrodes was recorded after amplification by a homemade amplifier (response time ~ 10 μs), which was equipped with a 0.033 Hz low cut filter to eliminate the baseline drift. To improve the S/N ratio, 30 laser pulses were used. The proteins adsorbed on ITO have random orientation [35]. Thus, the electrogeneity of the protein does not contribute to the potential difference, which purely reflects the local pH change due to the H^+ transfer reactions of the photolyzed proteins. The details of the apparatus were described elsewhere [35,36]. All measurements were performed at room temperature, ~25 °C.

3. Results and discussion

3.1. Genomic DNA sequence analysis

Ca. R. planktonica strain MWH-Dar1 is a red-pigmented actinobacterium isolated from a eutrophic pond in Tanzania [27]. In the previous study using degenerate polymerase chain reaction [23], ActR genes were identified in this strain (accession ID: FJ545219) and in the phylogenetically close strain MWH-Ta8 of *R. lacicola* described above (accession ID: FJ545221). Both strains belong to the actinobacterial Microbacteriaceae family and commonly have small cell sizes with diameters <0.5 μm and lengths <1.2 μm [27]. The strain MWH-Dar1 was present in a mixed culture with a small proportion (<1%) of a non-actinobacterial strain [27]. In this study, we initially repeated further purification cycles as described in the Materials and Methods section and established the pure culture. Then, the genomic DNA was isolated and sequenced, and

sequence analyses were performed. The genome size was 1.42 Mbp and the genome annotation revealed only 1366 putative open reading frames (ORFs). Thus, the genome of strain MWH-Dar1 is comparable in size and gene number to the genome of *R. lacicola* MWH-Ta8 (1.43 Mbp and 1408 ORFs) [38]. The 16S rRNA encoding gene found in the MWH-Dar1 genome was identical to the one determined previously (accession ID: AJ565415) [27]. MWH-Dar1 encodes only one microbial rhodopsin gene, corresponding to RpActR (accession ID: LC144836). Its 15th amino acid is Leu in the present genome sequencing but was replaced by His in the previous analysis using degenerate polymerase chain reaction [23]. As described above, *R. lacicola* lacks the gene encoding the β-carotene cleavage enzyme. On the other hand, a putative homolog of this enzyme is encoded in *Ca.* R. planktonica, together with other enzymes for retinal biosynthesis. These enzymes are listed in Table S1.

3.2. Structure of RpActR gene

Phylogenetically, ActRs belong to the xanthorhodopsin (XR)-like family of H^+ pumps [21], which is distinct from the PR-like family and characterized by a hypothesized binding pocket to accommodate the antenna carotenoids. This pocket is well studied in the H^+-pump XR from the cultivated eubacterium *Salinibacter ruber* [39,40] and its close relative *Gloeobacter* rhodopsin (GR) from the cyanobacterium *Gloeobacter violaceus* [41]. In contrast to ActRs, these host strains were isolated from a salt pond and calcareous rocks, respectively. XR and GR fall into subgroup I of the XR-like family [42]. ActRs are also categorized in subgroup I, but they form a noteworthy cluster by themselves [42].

RpActR shares high amino acid identity, 81%, with ActR of *R. lacicola* and moderately high values of 40% and 42% with XR and GR, respectively. Meanwhile, the identity with PR (21%), BR (19%) and a H^+ pump from eubacterium *Exiguobacterium sibiricum* (ESR) (29%) is relatively low. The sequence alignment of RpActR with BR, PR and XR is shown in Fig. S1. RpActR fully conserves essential amino acid residues for H^+-pumping function. During the photocycle, H^+ is sequentially transferred to higher-pKa residues, accompanied by pKa changes. This stepwise reaction is well studied in BR [43,44] and largely conserved in other H^+ pumps [2,19,20,45]. The first H^+ transfer reaction occurs during M intermediate formation, in which the H^+ of PSB is transferred to the superconserved Asp residue. This Asp is called the "H^+ acceptor" and corresponds to Asp85 in BR and Asp92 in RpActR. For BR, M intermediate formation also involves H^+ release to the extracellular (EC) medium. This H^+ is provided by the H^+-releasing group (PRG) consisting of Arg82, Glu194, Glu204, and water molecules located in the EC half channel. Arg82 is superconserved in H^+ pumps, while Glu194 and Glu204 are not fully conserved. This case also holds in RpActR, where Arg89 is conserved, but two Glu residues are replaced by Asn207 and Arg219 in RpActR, respectively. During the subsequent M to N intermediate transition, the deprotonated SB accepts H^+ from the "H^+ donor" residue, which corresponds to Asp96 in BR and is conserved as Glu in most H^+ pumps. Exceptionally, this residue is replaced by Lys in ESR [46]. For RpActR, the donor corresponds to Glu103. The last intermediate of the BR photocycle is O, which forms from N in association with two events: the H^+ uptake from the cytoplasmic (CP) medium by the donor residue and the reisomerization of retinal into its initial all-*trans* configuration. Then, O returns to its original state, which involves the deprotonation of the acceptor residue. In the case of BR, this H^+ moves to the deprotonated PRG.

The XR-like family conserves the hypothesized binding pocket for the antenna carotenoid as described above. Based on the crystal structure of XR, 16 residues are identified as forming this pocket [40,41]. The binding of the antenna carotenoid was also proven for GR, which conserves 11 residues [41]. Thus, not all residues identified in XR are essential for this binding. In RpActR, 10 residues are conserved (Fig. S1). Thus, RpActR probably conserves this binding ability. Similarly to *R. lacicola* [25], however, the host strain MWH-Dar1 lacks carotenoid ketolases, indicating that this strain does not contain keto-carotenoids, such as salinixanthin for XR and echinenone for GR.

3.3. Proton-pumping activity in native host cell

The functional expression of RpActR was examined through the light-induced pH change in the cell suspensions of MWH-Dar1, which was grown in the absence of exogenous retinal. As shown in Fig. 1, the cell suspensions showed distinct acidification upon light irradiation (trace a). This pH change was completely abolished by the addition of the protonophore CCCP (trace b), which eliminates the electrochemical gradient of H^+ across the cell membrane. Thus, the acidification was caused by active H^+ transport. This pH change also disappeared when the cells were grown in the presence of nicotine (trace c), which is known to inhibit the retinal biosynthesis pathway [47]. Thus, in the absence of nicotine, RpActR is functionally expressed in the retinal-bound form and causes the light-induced pH change. This functional expression was also confirmed based on ATP production. Fig. 2 shows the ATP level in MWH-Dar1, which was energy starved in the dark prior to the ATP assay. The cells before illumination contained approximately 1.5 nmol ATP per mg protein. This ATP level increased approximately threefold after 5 min illumination. Upon the addition of CCCP, this increase disappeared. For nicotine-grown cells, the illumination-induced increase did not occur even in the absence of CCCP. Thus, the functionally expressed RpActR creates the electrochemical gradient of H^+ across the cell membrane, which in turn drives ATP production. As described above, the actinobacterium *R. lacicola* also expressed ActR, but it did not exhibit light-induced activity due to the lack of retinal binding [25]. Thus, MWH-Dar1 is the first actinobacterium confirmed to perform ActR phototrophy. Meanwhile, we could not observe any apparent effect of illumination on the cell growth and the magnitudes of light-induced pH changes. Thus, further study is necessary to clarify the conditions inducing ActR expression and the cellular benefits derived from ActR phototrophy.

3.4. Spectroscopic characterization of the unphotolyzed state

Next, we cloned the RpActR gene and heterologously expressed it in *E. coli* cells in the presence of exogenous retinal. Reflecting the functional expression, the cells were colored pink, and their suspension showed light-induced acidification (data not shown). Using Ni-chelate chromatography, RpActR was purified and then used for functional characterization.

The purified RpActR shows an absorption maximum at 534 nm (Fig. 3A). In most microbial rhodopsins, the band near 280 nm has

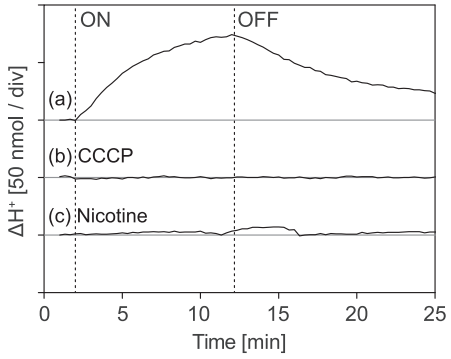

Fig. 1. Light-induced pH changes to the suspension of *Ca.* R. planktonica. The broken vertical lines indicate the beginning and end of green light illumination. The cells were suspended in unbuffered basal solution (0.3 g/L NaCl, 0.1 g/L $MgSO_4$). Traces a and b were obtained sequentially. After the measurement of trace a, 10 μM CCCP was added to the medium, and trace b was obtained. Trace c is the result for nicotine-grown cells in the absence of CCCP.

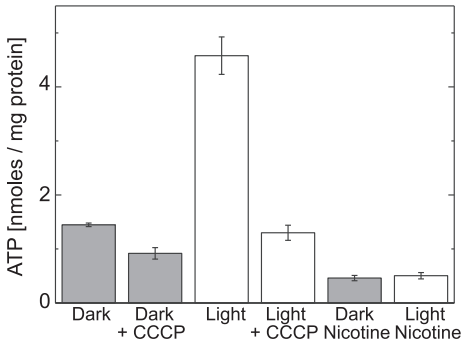

Fig. 2. The cellular ATP contents of *Ca.* R. planktonica. Energy-starved cells were suspended in 10 mM Tris-AcOH (pH 7.8) with and without 10 μM CCCP, then kept in the dark at room temperature. The cellular ATP contents were assayed without illumination (Dark) or after 5 min illumination (Light). The two bars labeled "Nicotine" are the results for the nicotine-grown cells. Each bar represents the mean ± SD ($n = 5$).

approximately 1.5-fold larger absorption than the retinal band in the visible region. In RpActR, however, these two bands have almost the same absorptions. This finding probably reflects lower Trp and/or Tyr content compared to other microbial rhodopsins. The Trp and Tyr contents are 3 and 12 for RpActR, 10 and 14 for PR, 5 and 15 for XR, and 8 and 11 for BR, respectively. The estimated molar extinction coefficients at 280 nm are 34,400 M^{-1} cm^{-1} for RpActR, 75,900 M^{-1} cm^{-1} for PR, 49,900 M^{-1} cm^{-1} for XR, and 60,400 M^{-1} cm^{-1} for BR, respectively. These were calculated by using the extinction coefficients of 5500 M^{-1} cm^{-1} for Trp and 1490 M^{-1} cm^{-1} for Tyr, respectively. Those explain the almost the same absorption between 280 nm and 534 nm.

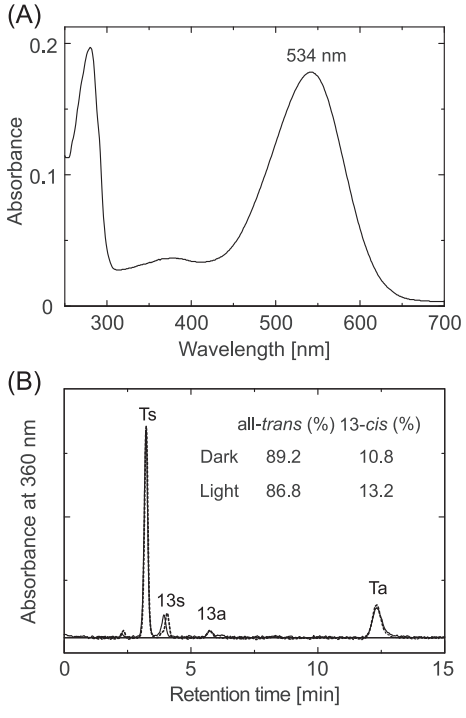

Fig. 3. Absorption spectrum and retinal isomer composition of RpActR. (A) Absorption spectrum of purified RpActR suspended in 50 mM Tris-HCl, pH 7.0, containing 300 mM NaCl and 0.1% DDM. (B) HPLC chromatographs of the retinal isomers extracted from RpActR, initially suspended in 10 mM MOPS, pH 7, containing 100 mM NaCl and 0.1% DDM. Ts, 13s, 13a and Ta denote retinal with all-*trans*/15-*syn*, 13-*cis*/15-*syn*, 13-*cis*/15-*anti* and all-*trans*/15-*anti* configurations, respectively. The chromatographic patterns were almost the same between light-adapted (solid line) and dark-adapted (broken line) RpActRs. The molar ratios of the retinal isomers were calculated from the peak areas.

The retinal isomer composition of RpActR was examined by HPLC analysis (Fig. 3B). For all ion pumps, only the photoisomerization from all-*trans* to 13-*cis* triggers the indispensable conformational changes for their respective ion translocations. However, only the archaeal ion pumps BR and HR also accommodate 13-*cis* retinal in their dark states, depending on light/dark adaptations [2]. In the light-adapted states after continuous illumination, they predominantly contain all-*trans* retinal. In the dark-adapted states after being kept in the dark, in contrast, the 13-*cis* contents increase by approximately 50%. As shown in Fig. 3B, RpActR contains predominantly all-*trans* retinal (~90%) under both conditions, for light and dark adaptations. Thus, compared to BR and HR, RpActR and other ion pumps probably accommodate retinal in relatively tight pockets that do not promote the 13-*cis* conformation.

Upon acidification, the H^+-acceptor residue is protonated, which is detectable by the spectral redshift for all H^+ pumps. Fig. 4A shows this spectral shift of RpActR. Upon protonation of the acceptor, RpActR showed a 34 nm redshift. In Fig. 4B, the absorbance change at 597 nm was plotted against pH. From this plot, the pKa of the acceptor (Asp92) was determined to be 5.8. This value is rather different from 2.6 for BR [43,44] but is similar to the members of the XR-like family: 6 for XR [48] and 4.5 for GR [49], respectively. Thus, RpActR appears to conserve the electrostatic interactions around the acceptor residue, which is characteristic of the XR-like H^+ pumps. However, RpActR showed different features from XR and GR in the influence of mutation on the donor residue. For GR, the acceptor pKa increases by at least 2 pH units up the mutation of E132Q (donor replacement by neutral residue) [49]. For BR and PR, the corresponding mutations (D96N for BR, E108Q for PR) have essentially no effects on their pKa values, probably due to the hydrophobic barriers surrounding the donor residues. Thus, compared to BR and PR, the donor of GR has unusually strong coupling with the acceptor regions. This coupling was also predicted for XR from its crystal structure [40], where the carboxyl of the donor Glu107 connects to the peptide carbonyl of Lys240, a residue binding the retinal, through a hydrogen-bonding network. To examine this coupling for RpActR, we made the donor mutant E103Q. The results are also plotted in Fig. 4B. This mutant showed almost the same pH dependence as the

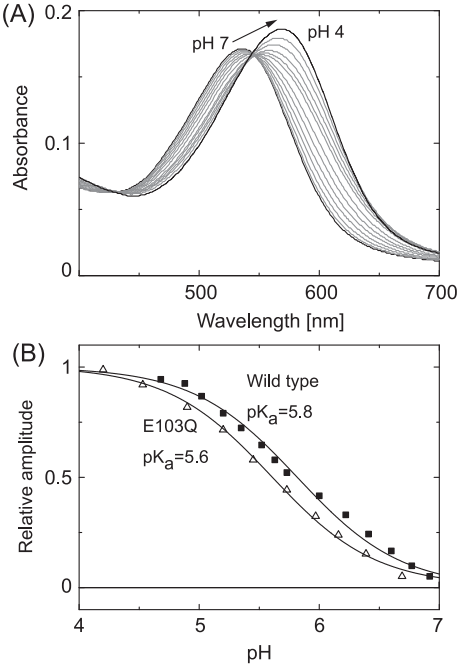

Fig. 4. Spectroscopic pH titrations to determine the pKa of Asp92. The spectral changes (A) and the relative amplitude changes at 597 nm (B). RpActR was suspended in 6-mix buffer containing 100 mM NaCl and 0.1% DDM. In (B), the results for the mutant E103Q are also shown. The pKa values were determined by fitting analyses using the Henderson-Hasselbalch equation.

wild-type RpActR. Consistently, the pKa determined of 5.6 for E103Q is very close to 5.8 for the wild-type RpActR. Thus, unlike XR and GR, RpActR shows only weak coupling between the donor and the acceptor, at least in the dark state.

3.5. Flash-induced absorbance changes

Next, we also examined the photoreaction of RpActR. The four large panels in Fig. 5 show the flash-induced absorbance changes measured at pH 6–9. As shown here, near physiological pH (pH 7), RpActR undergoes a relatively fast photocycle, which completes in approximately 100 ms. A fast photocycle is a common characteristic of ion-pumping rhodopsins. They transport one ion during a single photocycle. Thus, a faster photocycle can create a larger electrochemical potential gradient of the transported ion. The photocycle of RpActR is mainly characterized by the M intermediate at approximately 400 nm and subsequently forming intermediate at approximately 620 nm. In addition to these two wavelengths, the time-trace at 540 nm was plotted in each panel. This trace reflects the depletion and subsequent recovery of the original unphotolyzed state.

At pH 4, RpActR undergoes the photocycle lacking M, where only long-wavelength intermediate is observed. This is due to the protonation of acceptor residue in the dark. Reflecting the pKa of the acceptor residue (5.8), M becomes observable above pH 5. The yield of M increases by further pH increase, and then becomes saturated around pH 7. Interestingly, this M intermediate of RpActR has the fastest formation rate among the known microbial rhodopsins. Its formation was completed prior to 10 μs and could not be followed by our apparatus. The formation of M is associated with the fast H^+ transfer from the PSB to the acceptor, as described above. In the dark state, the acceptor has a lower pKa than PSB. Upon illumination, the pKa of the acceptor increases and becomes larger than the pKa of PSB. This inversion enables H^+ transfer from PSB to the acceptor during formation of M. For BR, the M formation rate depends on the interaction between the acceptor Asp85 and the neighboring Arg82 (corresponding to Arg89 of RpActR) [43]. The replacement of Arg82 with neutral residues induces both the acceleration of the M formation [50] and the elevation of the acceptor pKa from 2.6 to 7.2–7.5 [50,51]. Thus, the elevated pKa is considered to drive the fast H^+ transfer during M formation. For RpActR, the pKa of the acceptor (5.8) is higher than the pKa of BR (2.6) but still lower than the pKa of its Arg82 replacement mutants (7.2–7.5). For RpActR, therefore, the fast M formation could not be explained entirely by the pKa of the acceptor. The essential mechanism in RpActR should be clarified in future investigations.

The intermediate at 620 nm also shows characteristic behavior in its pH-dependent accumulation. Here, we tentatively name this intermediate P_{620}. Similar long-wavelength intermediates are also observed in all other H^+ pumps. They correspond to O intermediates for BR, XR and GR and to N intermediates for PR and ESR. Though the names are different, they commonly form after the H^+ uptake at the CP side by the donor residue. At high pH, the donor does not work well, and thus the formation of O (for BR, XR, and GR) and N (for PR and ESR) becomes substantially slow. Thus, their accumulation tends to become small and finally negligible as the pH increases. In contrast, for RpActR, the accumulation of P_{620} does not become negligible and remains prominent even at pH 10 (Figs. 5 and S2). This accumulation is probably caused by its prolonged decay above pH 8. P_{620} shows two- or three-phase decay. Above pH 8, the latter phase becomes prominent and slows down as pH increases. The decay of the preceding M also slows down as pH increases (Figs. 5 and S2). However, alkalization also retards the decay of P_{620}, and therefore the accumulation of P_{620} remains prominent.

To further examine the intermediates in the photocycle, we performed global fitting analyses of the flash-induced absorbance changes. All datasets measured at pH 6–9 were fitted adequately by a fitting equation of a sum of five exponential terms. This result indicates the existence of five kinetically defined states, which were designated as P_1–

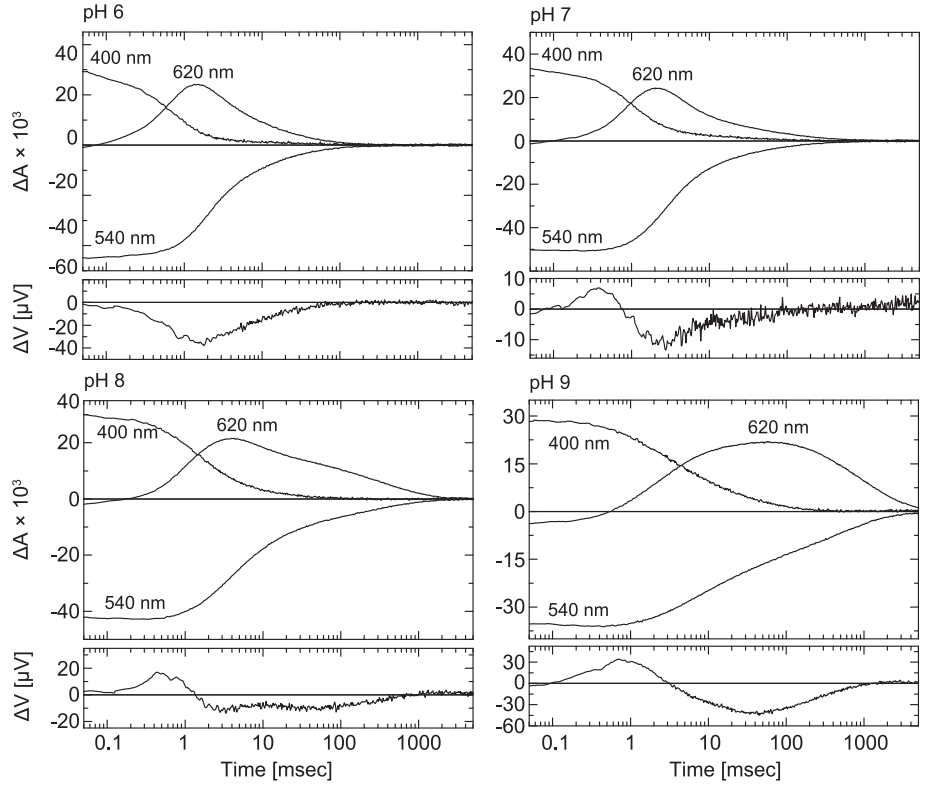

Fig. 5. The pH dependence of the RpActR photocycle. The photocycle was examined at four pH values (6–9) by flash-induced absorbance changes (large panels) and H^+ transfers measured using a transparent ITO electrode (thin panels), in which the H^+ release from RpActR is detected upon an upward shift of the electrode voltage, while the H^+ uptake is detected upon a downward shift. Egg-PC reconstituted RpActR was used in both experiments. The medium was 100 mM NaCl buffered with 6-mix buffer. The temperature was approximately 25 °C.

P_5. Using the fitting results, we calculated the spectra of the P_i states according to the sequential irreversible model. This model represents the photocycle by sequential reactions of kinetically defined P_i states, which may contain a few physically defined intermediates such as K, L, M, N and O [32]. The calculated spectra at pH 7 are shown in Fig. 6A, where P_0 denotes the spectrum of the original RpActR. The P_1 state contains the short-wavelength intermediate (λ_{max} ~ 410 nm), which corresponds to M. At approximately 500 nm, the P_1 spectrum has a small shoulder that might correspond to the preceding L intermediate, as it is very faint, reflecting the very fast formation of M. Upon the formation of P_2, the M content decreases slightly due to a small appearance of P_{620} in the longer-wavelength region. This P_{620} becomes dominant in the subsequent P_3 state. As described above, P_{620} shows multiphase decay, which is due to the contribution of P_{620} to the P_4 state: P_4 has a broad spectrum, probably reflecting the equilibrium between P_{620} and another intermediate whose spectrum is closely similar to the original state. The latter intermediate becomes the main component in the last P_5 state. This intermediate might be a precursor of the original state and could be assigned to RpActR′. Similar intermediates were also found in PR [52] and algal H^+ pumps [53,54]. Fig. 6B summarizes the photocycle of RpActR at pH 7 together with the decay time constants of the P_i states.

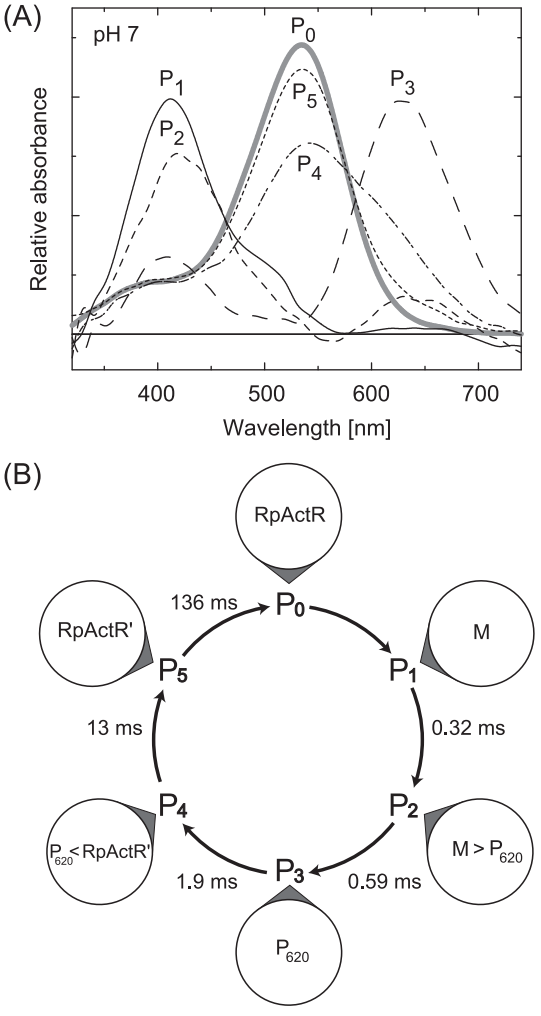

Fig. 6. Results of global fitting of the flash photolysis data. (A) Calculated absolute spectra of P_i states at pH 7 and 25 °C. P_0 denotes the original dark state of RpActR, whose spectrum was calculated by removing the scattering from the spectrum measured with a UV–visible spectrophotometer. (B) Proposed photocycle of RpActR at pH 7 and 25 °C. The decay time constants of the P_i states are also shown here. Each P_i state contains physically defined intermediates such as M, P_{620} and RpActR′. The P_2 and P_4 states contain the quasi-equilibrium between M and P_{620} and between P_{620} and RpActR′, respectively, where the signs ">" and "<" represent the differences in their contributions.

Essentially the same photocycle was observed between pH 6–9, although the decay time constants become slower with increasing pH. As described above and shown in Fig. 6B, the photocycle after 10 μs is characterized by only M, P_{620} and RpActR′.

3.6. Flash-induced proton transfers

Further insight into the photocycle was obtained from measurements using a transparent ITO electrode, which functions as a good time-resolved pH electrode [36,37]. The results are shown in the thin panels in Fig. 5, where the H^+ release and uptake are expressed as upward and downward voltage changes, respectively. As shown here, these H^+ transfer reactions are categorized into two patterns: one is observed at pH 6 and the other observed above pH 7.

At pH 6, the H^+ uptake and subsequent release occur almost simultaneously with the formation and decay of P_{620}. This behavior is the same as for O of PRG-disabled mutants of BR and wild-type GR, which also lacks the PRG, similarly to RpActR [49,55–57]. They do not release H^+ during the formation of M. Instead, they first capture H^+ with the donor residue during O formation. Subsequent O decay involves the deprotonation of the acceptor residue. This H^+ is predicted to be released to the EC medium. At pH 6, RpActR probably undergoes similar H^+ transfer reactions: that is, the first H^+ uptake by the donor residue during the P_{620} formation and the subsequent H^+ release from acceptor residue during the P_{620} decay. Thus, P_{620} could be assigned to O, although its retinal configuration is not yet confirmed. The first H^+ uptake is also observed in PR during N formation [55]. For PR, the formation of N involves two H^+ transfer reactions by the donor residue: the H^+ donation to the SB and the H^+ uptake from the CP medium. Thus, P_{620} is also similar to N of PR. However, for PR, the acceptor residue does not deprotonate during N decay but instead during the decay of the subsequent PR′ intermediate [55].

Above pH 7, on the other hand, the H^+ transfer signal becomes complicated: H^+ release occurs first despite the lack of PRG. Subsequently, the signal decreases below the baseline due to the H^+ uptake. Finally, the H^+ release occurs again, and the signal returns to the baseline. Unexpected first H^+ release is also observed in PR, which also lacks PRG, at alkaline pH [35,37]. However, the H^+ release in RpActR appears not to reflect the same reaction in PR. For PR, the first H^+ release is predicted to occur toward the CP medium, implying no contribution to the outward H^+ pumping activity [37]. For RpActR, the outward H^+-pumping activity reaches its maximum value at pH 7, a physiological pH (data not shown). This finding was confirmed by the light-induced pH change in the suspension of *E. coli* cells. Moreover, for PR, the first H^+ release is associated with the formation of another M intermediate, which forms in a branched photocycle appearing at alkaline pH [37]. This branch is observable above pH 8.5. Then, above pH 10, the branched photocycle becomes dominant, and the H^+ transfer reaction becomes simple: the H^+ release occurs first, and then the signal simply returns to the baseline due to the subsequent H^+ uptake. In contrast, for RpActR, photocycle branching does not seem to occur. As shown in Fig. 5, the first H^+ release begins to occur when the pH increases from 6 to 7. However, the essential difference in the photocycle does not occur at this pH increase. Similarly to the behavior at pH 6, the H^+ uptake above pH 7 occurs almost simultaneously with the formation of P_{620} despite the preceding H^+ release. This behavior implies that there exist two subpopulations of RpActR, both of which pumps H^+ outward: one undergoes the same H^+ transfer reactions observed at pH 6, where H^+ uptake occurs first upon P_{620} formation, followed by H^+ release upon P_{620} decay, while the other first releases H^+ on the EC side and then captures another H^+ on the CP side during the formation of P_{620}. Thus, there might exist a heterogeneity in RpActR that is not detectable in the photocycle kinetics but is detectable in the H^+ transfer sequences. Above pH 7, the first H^+ release occurs before the decay of the M intermediate. As described above, PRG-disabled mutants of BR show the first H^+ uptake. However, above pH 10, E194Q-containing mutants are

reported to show the first H^+ release from the acceptor residue during the M to N transition [58]. This behavior seems to resemble the case in RpActR. However, the protonation state of the acceptor residue is known to affect the absorption maximum. Despite the H^+ transfer sequence, RpActR undergoes a photocycle including M and P_{620}, as described above. Thus, for both H^+ transfer sequences, the acceptor residue should remain in the protonated state until the decay of P_{620}. The molecular origin of the heterogeneity and the residue performing the first H^+ release should be clarified in future investigations.

As described above, RpActR undergoes a photocycle consisting of M, P_{620} and RpActR′. P_{620} is probably assigned to O in GR and the PRG-disabled mutants of BR. Thus, N is not detectable in the RpActR photocycle. For BR, N accumulates when pH is higher than the pKa of the donor for H^+ uptake (7.5). At this alkaline pH, M and N are in a quasi-equilibrium state and thus decay together. This decay slows down as pH increases due to the slower H^+ uptake by the donor residue. For RpActR, the M decay becomes slower as pH increases (Fig. S2), which might reflect the delay in H^+ uptake by the donor residue. However, N is still not detectable in the alkaline pH, which might be caused by a fast N to M back reaction. At high pH, the H^+ uptake by the donor residue becomes the limiting process, and therefore M and N are in an equilibrium state. However, this equilibrium might shift substantially toward M due to the fast back reaction, which could cause negligible accumulation of N. On the other hand, the accumulation of P_{620} is still prominent at high pH because the decay of P_{620} becomes slower as pH increases. Why does the decay of P_{620} depend on pH? For sensory rhodopsin II from *Natronomonas pharaonis*, the O decay rate has been proven to depend on the pKa of the acceptor residue in a study involving many mutants [59]. This finding revealed that higher pKa results in slower O decay, which is rational because O decay is associated with the deprotonation of the acceptor residue. For RpActR, a certain residue might deprotonate above pH 8, which in turn elevates the pKa of the acceptor residue. Alternatively, the deprotonation of the residue might retard a conformational change that is indispensable for the deprotonation of the acceptor residue. The molecular factor determining P_{620} decay should be clarified in future investigation.

4. Conclusions

In this study, we present the first observation of ActR phototrophy in native actinobacterial cells. Without the help of exogenous retinal, RpActR showed light-induced H^+ pump activity and drove ATP production in its natural host cells. This result confirms the predicted significance of ActRs to the solar-energy inflow into freshwater ecosystems. Using the purified RpActR, we found several interesting features in the photocycle. M formation is extremely fast: It is competed before 10 μs and could not be followed by our apparatus. Compared to other H^+ pumps, there appears to be no specific difference in the residues surrounding both the PSB and the H^+ acceptor Asp92 (Fig. S1). Thus, the fast H^+ transfer between them might be caused by their specific coordination in the photolyzed state. After M formation, P_{620} and RpActR′ appear sequentially. P_{620} could be assigned to O in BR and other H^+ pumps. However, unlike conventional O, the decay of P_{620} shows pH-dependent retardation. This decay is probably governed by the protonation state of a certain residue. At pH 6, RpActR first captures H^+ during P_{620} formation and then releases H^+ during P_{620} decay. Above pH 7, approximately half of RpActR releases H^+ prior to uptake during P_{620} formation. The natural host of RpActR inhabits a pH-neutral freshwater pond. Thus, in the natural environment, RpActR probably shows heterogeneity in its H^+ transfer sequences. Does this heterogeneity confer a survival advantage to the cells in the freshwater environment? This question is an interesting topic for future investigation.

Transparency Document

The Transparency document associated with this article can be found, in the online version.

Acknowledgements

We thank Dr. S. Takiya for allowing us to use the luminometer and for helpful discussions. This work was supported by JSPS KAKENHI to T.K. (26440042) and M.D. (16K14044).

Appendix A. Supplementary data

Supplementary data to this article can be found online at http://dx.doi.org/10.1016/j.bbabio.2016.09.006.

References

[1] J. Heberle, X. Deupi, G. Schertler, Retinal proteins - you can teach an old dog new tricks, Biochim. Biophys. Acta 1837 (2014) 531–532.
[2] O.P. Ernst, D.T. Lodowski, M. Elstner, P. Hegemann, L.S. Brown, H. Kandori, Microbial and animal rhodopsins: structures, functions, and molecular mechanisms, Chem. Rev. 114 (2014) 126–163.
[3] D. Oesterhelt, W. Stoeckenius, Rhodopsin-like protein from the purple membrane of *Halobacterium halobium*, Nature 233 (1971) 149–152.
[4] D. Oesterhelt, W. Stoeckenius, Functions of a new photoreceptor membrane, Proc. Natl. Acad. Sci. U. S. A. 70 (1973) 2853–2857.
[5] A. Matsuno-Yagi, Y. Mukohata, Two possible roles of bacteriorhodopsin; a comparative study of strains of *Halobacterium halobium* differing in pigmentation, Biochem. Biophys. Res. Commun. 78 (1977) 237–243.
[6] R.A. Bogomolni, J.L. Spudich, Identification of a third rhodopsin-like pigment in phototactic *Halobacterium halobium*, Proc. Natl. Acad. Sci. U. S. A. 79 (1982) 6250–6254.
[7] T. Takahashi, H. Tomioka, N. Kamo, Y. Kobatake, A photosystem other than PS370 also mediates the negative phototaxis of *Halobacterium halobium*, FEMS Microbiol. Lett. 28 (1985) 161–164.
[8] M. Grote, M.A. O'Malley, Enlightening the life sciences: the history of halobacterial and microbial rhodopsin research, FEMS Microbiol. Rev. 35 (2011) 1082–1099.
[9] K.H. Jung, New type of cation pumping microbial rhodopsins in marine bacteria, 244th ACS National Meeting & Exposition, Philadelphia, PA 2012, p. 271 (Abstract).
[10] K. Inoue, H. Ono, R. Abe-Yoshizumi, S. Yoshizawa, H. Ito, K. Kogure, H. Kandori, A light-driven sodium ion pump in marine bacteria, Nat. Commun. 4 (2013) 1678.
[11] O.A. Sineshchekov, K.H. Jung, J.L. Spudich, Two rhodopsins mediate phototaxis to low-and high-intensity light in *Chlamydomonas reinhardtii*, Proc. Natl. Acad. Sci. U. S. A. 99 (2002) 8689.
[12] G. Nagel, D. Ollig, M. Fuhrmann, S. Kateriya, A.M. Musti, E. Bamberg, P. Hegemann, Channelrhodopsin-1: a light-gated proton channel in green algae, Science 296 (2002) 2395.
[13] G. Nagel, T. Szellas, W. Huhn, S. Kateriya, N. Adeishvili, P. Berthold, D. Ollig, P. Hegemann, E. Bamberg, Channelrhodopsin-2, a directly light-gated cation-selective membrane channel, Proc. Natl. Acad. Sci. U. S. A. 100 (2003) 13940.
[14] E.G. Govorunova, O.A. Sineshchekov, R. Janz, X. Liu, J.L. Spudich, Natural light-gated anion channels: a family of microbial rhodopsins for advanced optogenetics, Science 349 (2015) 647–650.
[15] K.-H. Jung, V.D. Trivedi, J.L. Spudich, Demonstration of a sensory rhodopsin in eubacteria, Mol. Microbiol. 47 (2003) 1513–1522.
[16] O. Béjà, L. Aravind, E.V. Koonin, M.T. Suzuki, A. Hadd, L.P. Nguyen, S.B. Jovanovich, C.M. Gates, R.A. Feldman, J.L. Spudich, E.N. Spudich, E.F. DeLong, Bacterial rhodopsin: evidence for a new type of phototrophy in the sea, Science 289 (2000) 1902–1906.
[17] O. Béjà, E.N. Spudich, J.L. Spudich, M. Leclerc, E.F. DeLong, Proteorhodopsin phototrophy in the ocean, Nature 411 (2001) 786–789.
[18] O. Béjà, J. Pinhassi, J.L. Spudich, Proteorhodopsins: Widespread Microbial Light-Driven Proton Pumps, in: S.A. Levin (Ed.), Encyclopedia of Biodiversity, Elsevier, New York 2013, pp. 280–285.
[19] L.S. Brown, Eubacterial rhodopsins - unique photosensors and diverse ion pumps, Biochim. Biophys. Acta 1837 (2014) 553–561.
[20] K. Inoue, Y. Kato, H. Kandori, Light-driven ion-translocating rhodopsins in marine bacteria, Trends Microbiol. 23 (2014) 91–98.
[21] A.K. Sharma, O. Zhaxybayeva, R.T. Papke, W.F. Doolittle, Actinorhodopsins: proteorhodopsin like gene sequences found predominantly in non-marine environments, Environ. Microbiol. 10 (2008) 1039–1056.
[22] F. Warnecke, R. Amann, J. Pernthaler, Actinobacterial 16S rRNA genes from freshwater habitats cluster in four distinct lineages, Environ. Microbiol. 6 (2004) 242–253.
[23] A.K. Sharma, K. Sommerfeld, G.S. Bullerjahn, A.R. Matteson, S.W. Wilhelm, J. Jezbera, U. Brandt, W.F. Doolittle, M.W. Hahn, Actinorhodopsin genes discovered in diverse freshwater habitats and among cultivated freshwater *Actinobacteria*, ISME J. 3 (2009) 726–737.
[24] M. Martinez-Garcia, B.K. Swan, N.J. Poulton, M.L. Gomez, D. Masland, M.E. Sieracki, R. Stepanauskas, High-throughput single-cell sequencing identifies photoheterotrophs and chemoautotrophs in freshwater bacterioplankton, ISME J. 6 (2012) 113–123.

[25] J.L. Keffer, M.W. Hahn, J.A. Maresca, Characterization of an unconventional rhodopsin from the freshwater actinobacterium *Rhodoluna lacicola*, J. Bacteriol. 197 (2015) 2704–2712.
[26] M.W. Hahn, P. Stadler, Q.L. Wu, M. Pockl, The filtration-acclimatization method for isolation of an important fraction of the not readily cultivable bacteria, J. Microbiol. Methods 57 (2004) 379–390.
[27] M.W. Hahn, Description of seven candidate species affiliated with the phylum *Actinobacteria*, representing planktonic freshwater bacteria, Int. J. Syst. Evol. Microbiol. 59 (2009) 112–117.
[28] R.K. Aziz, D. Bartels, A.A. Best, M. DeJongh, T. Disz, R.A. Edwards, K. Formsma, S. Gerdes, E.M. Glass, M. Kubal, F. Meyer, G.J. Olsen, R. Olson, A.L. Osterman, R.A. Overbeek, L.K. McNeil, D. Paarmann, T. Paczian, B. Parrello, G.D. Pusch, C. Reich, R. Stevens, O. Vassieva, V. Vonstein, A. Wilke, O. Zagnitko, The RAST Server: rapid annotations using subsystems technology, BMC Genomics 9 (2008) 75.
[29] T. Hasemi, T. Kikukawa, N. Kamo, M. Demura, Characterization of a cyanobacterial chloride-pumping rhodopsin and its conversion into a proton pump, J. Biol. Chem. 291 (2016) 355–362.
[30] Y. Yamashita, T. Kikukawa, T. Tsukamoto, M. Kamiya, T. Aizawa, K. Kawano, S. Miyauchi, N. Kamo, M. Demura, Expression of *salinarum* halorhodopsin in *Escherichia coli* cells: solubilization in the presence of retinal yields the natural state, Biochim. Biophys. Acta 1808 (2011) 2905–2912.
[31] M. Sato, M. Kubo, T. Aizawa, N. Kamo, T. Kikukawa, K. Nitta, M. Demura, Role of putative anion-binding sites in cytoplasmic and extracellular channels of *Natronomonas pharaonis* halorhodopsin, Biochemistry 44 (2005) 4775–4784.
[32] I. Chizhov, D.S. Chernavskii, M. Engelhard, K.H. Mueller, B.V. Zubov, B. Hess, Spectrally silent transitions in the bacteriorhodopsin photocycle, Biophys. J. 71 (1996) 2329–2345.
[33] C. Hasegawa, T. Kikukawa, S. Miyauchi, A. Seki, Y. Sudo, M. Kubo, M. Demura, N. Kamo, Interaction of the halobacterial transducer to a halorhodopsin mutant engineered so as to bind the transducer: Cl^- circulation within the extracellular channel, Photochem. Photobiol. 83 (2007) 293–302.
[34] T. Kikukawa, C. Kusakabe, A. Kokubo, T. Tsukamoto, M. Kamiya, T. Aizawa, K. Ihara, N. Kamo, M. Demura, Probing the Cl^--pumping photocycle of *pharaonis* halorhodopsin: examinations with bacterioruberin, an intrinsic dye, and membrane potential-induced modulation of the photocycle, Biochim. Biophys. Acta 1847 (2015) 748–758.
[35] J. Tamogami, T. Kikukawa, S. Miyauchi, E. Muneyuki, N. Kamo, A tin oxide transparent electrode provides the means for rapid time-resolved pH measurements: application to photoinduced proton transfer of bacteriorhodopsin and proteorhodopsin, Photochem. Photobiol. 85 (2009) 578–589.
[36] L. Reissig, T. Iwata, T. Kikukawa, M. Demura, N. Kamo, H. Kandori, Y. Sudo, Influence of halide binding on the hydrogen bonding network in the active site of *Salinibacter* sensory rhodopsin I, Biochemistry 51 (2012) 8802–8813.
[37] J. Tamogami, K. Sato, S. Kurokawa, T. Yamada, T. Nara, M. Demura, S. Miyauchi, T. Kikukawa, E. Muneyuki, N. Kamo, Formation of M-like intermediates in proteorhodopsin in alkali solutions (pH ≧ ~8.5) where the proton release occurs first in contrast to the sequence at lower pH, Biochemistry (2016).
[38] M.W. Hahn, J. Schmidt, S.J. Taipale, W.F. Doolittle, U. Koll, *Rhodoluna lacicola* gen. nov., sp. nov., a planktonic freshwater bacterium with stream-lined genome, Int. J. Syst. Evol. Microbiol. 64 (2014) 3254–3263.
[39] S.P. Balashov, E.S. Imasheva, V.A. Boichenko, J. Anton, J.M. Wang, J.K. Lanyi, Xanthorhodopsin: a proton pump with a light-harvesting carotenoid antenna, Science 309 (2005) 2061–2064.
[40] H. Luecke, B. Schobert, J. Stagno, E.S. Imasheva, J.M. Wang, S.P. Balashov, J.K. Lanyi, Crystallographic structure of xanthorhodopsin, the light-driven proton pump with a dual chromophore, Proc. Natl. Acad. Sci. U. S. A. 105 (2008) 16561–16565.
[41] E.S. Imasheva, S.P. Balashov, A.R. Choi, K.H. Jung, J.K. Lanyi, Reconstitution of *Gloeobacter violaceus* rhodopsin with a light-harvesting carotenoid antenna, Biochemistry 48 (2009) 10948–10955.
[42] J. Vollmers, S. Voget, S. Dietrich, K. Gollnow, M. Smits, K. Meyer, T. Brinkhoff, M. Simon, R. Daniel, Poles apart: Arctic and Antarctic *Octadecabacter* strains share high genome plasticity and a new type of xanthorhodopsin, PLoS One 8 (2013), e63422.
[43] S.P. Balashov, Protonation reactions and their coupling in bacteriorhodopsin, Biochim. Biophys. Acta 1460 (2000) 75–94.
[44] J.K. Lanyi, Bacteriorhodopsin, Annu. Rev. Physiol. 66 (2004) 665–688.
[45] L.E. Petrovskaya, S.P. Balashov, E.P. Lukashev, E.S. Imasheva, I.Y. Gushchin, A.K. Dioumaev, A.B. Rubin, D.A. Dolgikh, V.I. Gordeliy, J.K. Lanyi, M.P. Kirpichnikov, ESR - a retinal protein with unusual properties from *Exiguobacterium sibiricum*, Biochemistry (Mosc.) 80 (2015) 688–700.
[46] L.E. Petrovskaya, E.P. Lukashev, V.V. Chupin, S.V. Sychev, E.N. Lyukmanova, E.A. Kryukova, R.H. Ziganshin, E.V. Spirina, E.M. Rivkina, R.A. Khatypov, L.G. Erokhina, D.A. Gilichinsky, V.A. Shuvalov, M.P. Kirpichnikov, Predicted bacteriorhodopsin from *Exiguobacterium sibiricum* is a functional proton pump, FEBS Lett. 584 (2010) 4193–4196.
[47] C.D. Howes, P.P. Batra, Accumulation of lycopene and inhibition of cyclic carotenoids in *Mycobacterium* in the presence of nicotine, Biochim. Biophys. Acta 222 (1970) 174–179.
[48] E.S. Imasheva, S.P. Balashov, J.M. Wang, J.K. Lanyi, pH-dependent transitions in xanthorhodopsin, Photochem. Photobiol. 82 (2006) 1406–1413.
[49] M.R. Miranda, A.R. Choi, L. Shi, A.G. Bezerra Jr., K.-H. Jung, L.S. Brown, The photocycle and proton translocation pathway in a cyanobacterial ion-pumping rhodopsin, Biophys. J. 96 (2009) 1471–1481.
[50] S.P. Balashov, R. Govindjee, M. Kono, E. Imasheva, E. Lukashev, T.G. Ebrey, R.K. Crouch, D.R. Menick, Y. Feng, Effect of the arginine-82 to alanine mutation in bacteriorhodopsin on dark adaptation, proton release, and the photochemical cycle, Biochemistry 32 (1993) 10331–10343.
[51] L.S. Brown, L. Bonet, R. Needleman, J.K. Lanyi, Estimated acid dissociation constants of the Schiff base, Asp-85, and Arg-82 during the bacteriorhodopsin photocycle, Biophys. J. 65 (1993) 124–130.
[52] G. Váró, L.S. Brown, M. Lakatos, J.K. Lanyi, Characterization of the photochemical reaction cycle of proteorhodopsin, Biophys. J. 84 (2003) 1202–1207.
[53] T. Kikukawa, K. Shimono, J. Tamogami, S. Miyauchi, S.Y. Kim, T. Kimura-Someya, M. Shirouzu, K.H. Jung, S. Yokoyama, N. Kamo, Photochemistry of *Acetabularia* rhodopsin II from a marine plant, *Acetabularia acetabulum*, Biochemistry 50 (2011) 8888–8898.
[54] M. Furuse, J. Tamogami, T. Hosaka, T. Kikukawa, N. Shinya, M. Hato, N. Ohsawa, S.Y. Kim, K.H. Jung, M. Demura, S. Miyauchi, N. Kamo, K. Shimono, T. Kimura-Someya, S. Yokoyama, M. Shirouzu, Structural basis for the slow photocycle and late proton release in *Acetabularia* rhodopsin I from the marine plant *Acetabularia acetabulum*, Acta Crystallogr. D Biol. Crystallogr. 71 (2015) 2203–2216.
[55] A.K. Dioumaev, L.S. Brown, J. Shih, E.N. Spudich, J.L. Spudich, J.K. Lanyi, Proton transfers in the photochemical reaction cycle of proteorhodopsin, Biochemistry 41 (2002) 5348–5358.
[56] S.P. Balashov, E.S. Imasheva, T.G. Ebrey, N. Chen, D.R. Menick, R.K. Crouch, Glutamate-194 to cysteine mutation inhibits fast light-induced proton release in bacteriorhodopsin, Biochemistry 36 (1997) 8671–8676.
[57] A.K. Dioumaev, H.T. Richter, L.S. Brown, M. Tanio, S. Tuzi, H. Saito, Y. Kimura, R. Needleman, J.K. Lanyi, Existence of a proton transfer chain in bacteriorhodopsin: participation of Glu-194 in the release of protons to the extracellular surface, Biochemistry 37 (1998) 2496–2506.
[58] T. Lazarova, C. Sanz, E. Querol, E. Padrós, Fourier transform infrared evidence for early deprotonation of Asp85 at alkaline pH in the photocycle of bacteriorhodopsin mutants containing E194Q, Biophys. J. 78 (2000) 2022–2030.
[59] M. Iwamoto, Y. Sudo, K. Shimono, T. Araiso, N. Kamo, Correlation of the O-intermediate rate with the pKa of Asp-75 in the dark, the counterion of the Schiff base of pharaonis phoborhodopsin (sensory rhodopsin II), Biophys. J. 88 (2005) 1215–1223.